OPEN ACCESS

A novel method achieving ultra-high geometrical resolution in scanning tunnelling microscopy

New Journal of Physics
The open–access journal for physics

A novel method achieving ultra-high geometrical resolution in scanning tunnelling microscopy

R Temirov[1,2], S Soubatch[1,2], O Neucheva[1,2], A C Lassise[2] and F S Tautz[1,2,3]

[1] Institut für Bio- und Nanosysteme 3, JARA, Forschungszentrum Jülich, 52425 Jülich, Germany
[2] School of Engineering and Science, Jacobs University, P O Box 750561, 28725 Bremen, Germany
E-mail: s.tautz@fz-juelich.de

New Journal of Physics **10** (2008) 053012 (11pp)
Received 8 February 2008
Published 12 May 2008
Online at http://www.njp.org/
doi:10.1088/1367-2630/10/5/053012

Abstract. We report a new contrast mechanism in which scanning tunnelling micrographs of a certain class of molecules resemble chemists' structure formulae. The method is based on adding molecular hydrogen below its condensation temperature to the tunnelling junction of a low-temperature scanning tunnelling microscope. In the presence of hydrogen, the scanning tunnelling microscope contrast can be switched between the conventional mapping of the electronic local density of states and the new geometric imaging by selecting the appropriate bias voltage. Scanning tunnelling spectroscopy suggests that the coupling of the electron tunnelling current to an internal degree of freedom in the tunnelling junction is responsible for the geometric contrast. The new scanning tunnelling hydrogen microscopy (STHM) allows the chemical identification of certain molecular species by their structure.

Scanning tunnelling microscopy (STM) is a powerful tool for studying the structural [1], electronic [2], vibrational [3] and transport [4, 5] properties of complex adsorbates on a single-molecule scale. A major disadvantage of the method is its lack of chemical sensitivity, which would allow the direct identification of molecular species. In this paper, we demonstrate that low-temperature STM in the presence of condensed molecular hydrogen resolves the geometric structure of planar organic adsorbate molecules on metal surfaces. Because the images that are obtained with this technique closely resemble chemists' structure formulae, the geometric

[3] Author to whom any correspondence should be addressed.

imaging mode of *scanning tunnelling hydrogen microscopy* (STHM) can be considered as a new type of 'chemical' resolution for the scanning tunnelling microscope. To make the STM chemically sensitive, a range of local spectroscopic approaches have been suggested, including the measurement of (i) the valence electronic structure in scanning tunnelling spectroscopy (STS) [2, 6], (ii) optical spectra derived from tip-induced electroluminescence (the so-called single-molecule fluorescence experiments) [7, 8] and (iii) single-molecule vibrational spectra in inelastic tunnelling spectroscopy (IETS) [3], [9]–[11]. However, in spite of some success in all three approaches, true and universal chemical sensitivity for the STM has not yet been achieved. In this situation, the ultra-high resolution geometric imaging mode of STHM offers a complementary approach.

To illustrate the new technique, we focus on two flat, platelet-like molecules, namely 3,4,9,10-perylene-tetracarboxylic-dianhydride (PTCDA) and tetracene (cf the supplement, available from stacks.iop.org/NJP/10/053012/mmedia), but the method should be extendable to a much broader class of molecules, including e.g. C_{60} or even graphene layers. The key notion is sensitizing the tunnelling junction with molecular hydrogen below the latter's condensation temperature ($T_{\mathrm{cond}} = 20.28\,\mathrm{K}$, $T_{\mathrm{melt}} = 14.01\,\mathrm{K}$)[4]. Experiments with molecular deuterium have also been conducted and yield similar results as for hydrogen.

Hydrogen sensitization of the STM junction was achieved by flooding the chamber in which the cold ($\sim 10\,\mathrm{K}$) STM is located with molecular hydrogen of purity 99.999%. Hydrogen pressures were varied in the range of 10^{-9}–10^{-7} mbar. The pressure is measured by an ion gauge outside the two closed cryoshields of the STM (the outer at LN_2, the latter at LHe temperatures). In this pressure range, the sensitization has been reproducibly achieved. In our experiments, the hydrogen coverage has not been characterized quantitatively. However, during hydrogen exposure, scanning tunnelling spectra are constantly recorded. As soon as the first signs of hydrogen in the junction appear (cf below) the exposure is stopped. This method reliably allows a reproducible tip sensitization on the three different surfaces that we have tried (Ag(111), Ag(110) and Au(111)). In addition to the controlled procedure described above, several instances of unintentional hydrogen deposition have been registered, caused by the degassing of the LHe cryostat. The uncontrolled hydrogen deposition produces the same effect as the regular deposition procedure described above.

Tungsten wire of 0.5 mm diameter, electrochemically etched in KOH, has been used for the STM tips. The tip was cleaned by argon sputtering (2 kV) for 15 min, at pressures around 10^{-5} mbar. After annealing for 2 min, the tip was transferred into the cold STM. Finally, it was prepared by indentation into the clean metal substrates. Tip quality has been validated by measuring the surface states of Ag(111) or Au(111), or the known molecular electronic structure [12]. STM images are displayed using the WSxM program [13].

The second row in figure 1 displays several constant current images recorded under hydrogen-sensitized conditions. The effect of hydrogen sensitization is observed as a drastically different image contrast at low bias voltages as compared with conventional local density of states images displayed in the first row of figure 1. All data in figure 1 (except figures 1(a)–(c)) were obtained as a result of controlled hydrogen deposition. The images shown in figures 1(a)–(c) were measured after uncontrolled hydrogen deposition. Comparing the resolution of the sensitized STM junction with the structure formulae of the imaged compounds (displayed in the bottom row of figure 1) reveals that in all the cases considered here, the addition

[4] http://www.webelements.com.

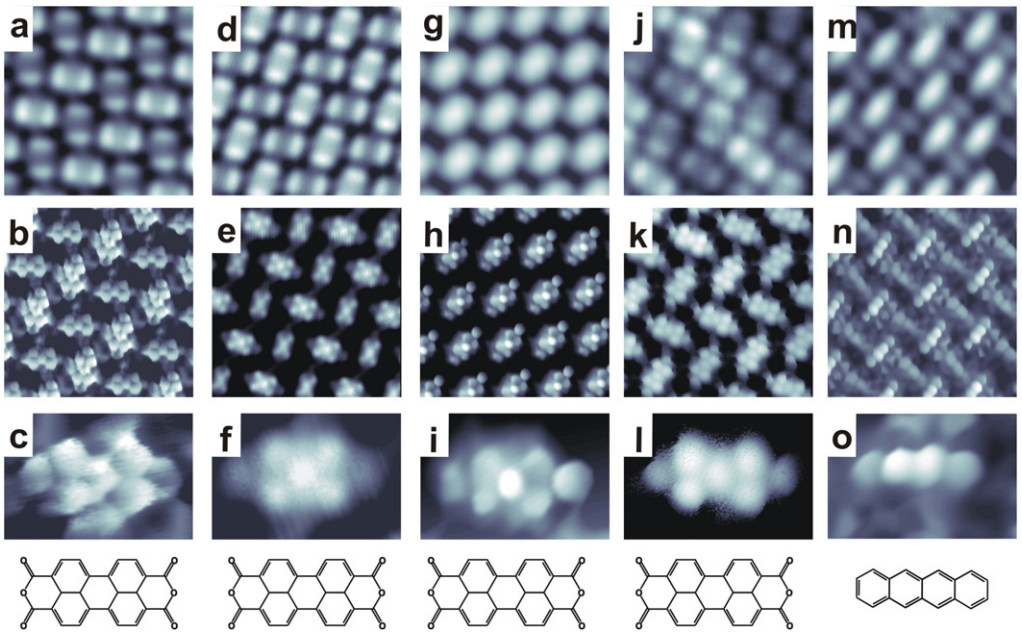

Figure 1. Set of images obtained on organic monolayers with hydrogen-sensitized STM tips. Images (a)–(c) were obtained after unintentional hydrogen deposition (cf text). Images (d)–(o) were measured after dosing of molecular hydrogen in the STM chamber, following the procedure described in the text. Images in the first two rows have a size of $5 \times 5\,\mathrm{nm}^2$. Images in the third row have a size of $1 \times 1.5\,\mathrm{nm}^2$. Images (a)–(f) were measured on PTCDA/Ag(111), (g)–(i) on PTCDA/Ag(110), (j)–(l) on PTCDA/Au(111) and (m)–(o) on tetracene/Ag(110). First row: electronic resolution obtained with hydrogen-sensitized tips at bias voltages (modulus) higher than 0.30 V. Second and third rows: geometric resolution obtained with STHM at bias voltages (modulus) lower than or equal to 0.030 V. Last row: chemical structure formulae of the corresponding molecules. Tunnelling parameters: (a) 2.1 nA, −0.340 V, (b) and (c) 2.1 nA, −0.015 V, (d) 0.5 nA, −0.340 V, (e) and (f) 0.5 nA, −0.030 V, (g) 1.0 nA, −0.340 V, (h) and (i) 1.0 nA, −0.010 V, (j) 0.03 nA, 1.4 V, (k) and (l) 0.03 nA, −0.020 V, (m) 1.0 nA, −0.340 V, (n) and (o) 1.0 nA, −0.010 V.

of hydrogen yields images of the *chemical* or *geometric* structure (in the following, simply called geometric structure) rather than the *electronic* structure of the molecule. In particular, we note that the geometric contrast mechanism images the ring structure of the molecules.

Figure 1 also demonstrates that the hydrogen-sensitized STM junction, while capable of a new type of resolution, at the same time preserves the ability to image the electronic structure of the adsorbate: all *geometric* images have been recorded at low bias voltages of approximately ±10–30 mV, while at higher positive or negative bias voltages the conventional electronic contrast reappears (figures 1(a), (d), (g), (j) and (m)). It is possible to switch between the two contrasts repeatedly by changing the bias voltage. Moreover, the data in figure 1 indicate that the geometric contrast shows no dependence on the substrate or on the interface electronic structure, which varies appreciably between the interfaces considered here (see the supplement, available

from stacks.iop.org/NJP/10/053012/mmedia, for more details). Finally, figure 1 demonstrates that the sensitized junction achieves geometric resolution on the two different molecules that we have tried.

Figure 1 also provides a first impression of the potential of the new imaging technique: on the Ag(110) surface (figures 1(g), (h), (i), (m), (n) and (o)) the strong interaction of both PTCDA and tetracene with the metal prevents the resolution of molecular orbitals and indeed *any* internal molecular structure in the conventional imaging regime. This is a well-known effect that requires the use of weakly interacting insulating substrates if high-resolution (electronic) molecular images are desired [2]. In the new mechanism, this restriction does not arise: the geometric resolution on the more strongly interacting Ag(110) surface is no worse than on Ag(111) or Au(111). Moreover, our example of tetracene/Ag(110) demonstrates that the geometric imaging method has the potential of revealing unknown structures: from the electronic image of figure 1(m) alone, the existence of more than one type of tetracene molecule within the structure cannot be inferred, while the STHM image in figure 1(n) reveals at least two different types of tetracene molecules. Finally, we note that not only the internal molecular structure is imaged. In figure 2(b), a constant height $\mathrm{d}I/\mathrm{d}V$ image (recorded at zero bias) of the PTCDA/Ag(111) interface is displayed, together with the calculated structure of the molecular layer. One clearly observes image features between the molecules in the region where intermolecular H-bonds are expected (or where the atoms of neighbouring molecules form ring-like structures).

In an effort to rationalize the geometric image contrast, one of the first questions to be asked is: where is the hydrogen adsorbed and how much of it is present? Most probably hydrogen adsorbs on the cold surface as well as on the cold tip, but the amount of hydrogen present on the surface (and the tip) during STHM imaging is not known. It turns out, however, that the hydrogen coverage is not critical and the geometric contrast can be observed in a rather broad range of coverages, as long as a certain critical coverage is surpassed. The data moreover suggest that the sensitization already appears at coverage equivalents below a full monolayer. This conclusion is based on several experiments with low exposures. In such cases, it was repeatedly observed that the geometric contrast spontaneously switched to the conventional electronic one, but on a timescale of minutes the geometric contrast was spontaneously restored; in the case of the unintentional deposition mentioned above (figures 1(a)–(c), presumably a very low coverage), the modified contrast even did not restore at all after it had disappeared due to a tip crash. The above observations indicate that the geometric resolution is caused by a hydrogen-modified junction rather than by a complete decoration of the molecular layer with hydrogen.

The next question is: in what form (molecular, atomic, or ionic (= proton)) is hydrogen present in the STHM junction? Experiments suggest that molecular hydrogen is responsible for the geometric imaging effect: firstly, the effect disappears at temperatures higher than 25 K, which corresponds to the desorption temperature of molecular hydrogen. Secondly, we have never observed any etching of the sensitive organic layers, which may be expected if atomic hydrogen was present [14], and thirdly, it is known that on single-crystal Ag surfaces no dissociation of hydrogen occurs [15]. Although there are some experimental indications that support a cluster of hydrogen picked up successively by the tip during scanning, rather than a single molecule (e.g. the time evolution of the spectra to be discussed below), it is not clear whether the sensitizing hydrogen probe consists of a single molecule or a cluster. *If* we have a cluster of molecular hydrogen, one may wonder whether it is present in the liquid or solid state. The base temperature of our STM (10 K) is close to the melting point of hydrogen

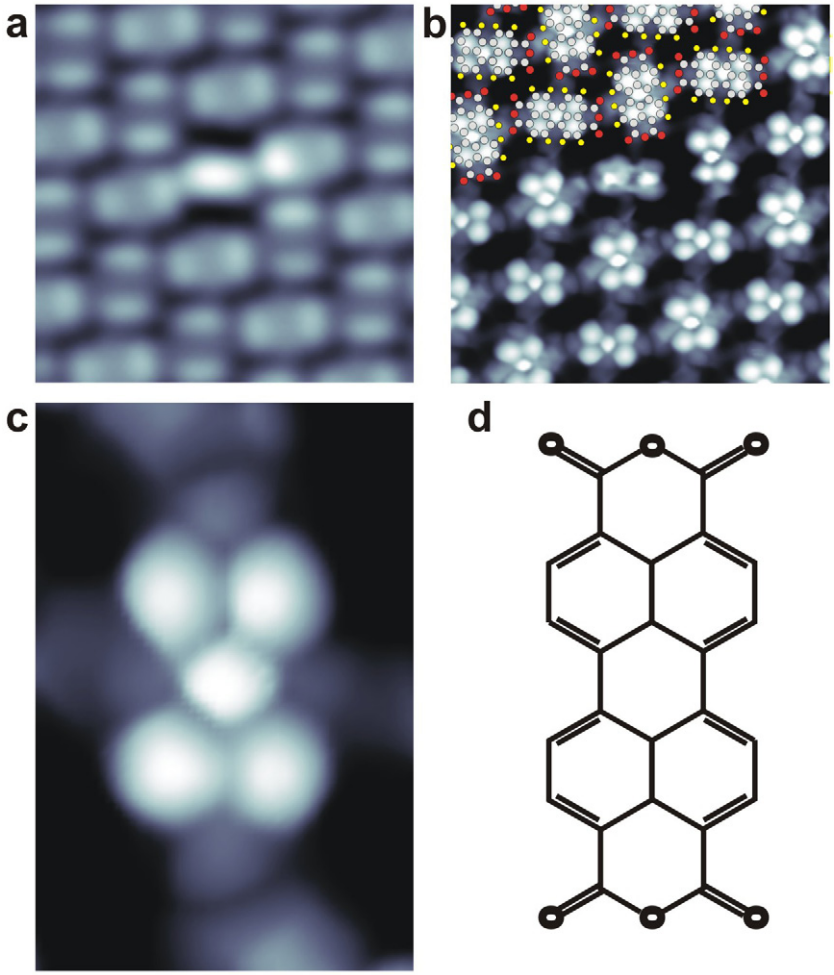

Figure 2. Spectroscopic imaging of PTCDA/Ag(111) in the geometric mode. The STM tip is sensitized with deuterium. (a) $5 \times 5\,\mathrm{nm}^2$ conventional constant current image of the electronic local density of states, recorded with 1 nA, -0.340 V. In the centre of the image a point defect (impurity molecule) is visible. (b) $5 \times 5\,\mathrm{nm}^2$ constant height $\mathrm{d}I/\mathrm{d}V$ image of the area shown in (a), recorded in the geometric imaging mode. Prior to recording the image, the tip was stabilized at 1 nA, -0.010 V and then the bias voltage was set to 0. Modulation amplitude, 4 mV; modulation frequency, 626 Hz. In the upper left part of the image, the calculated atomic structure of a PTCDA layer on Ag(111), taken from [6], is superimposed. Grey, carbon; red, oxygen; yellow, hydrogen. (c) Enlarged section of (b), $1 \times 1.5\,\mathrm{nm}^2$. (d) Structural formula of PTCDA.

(14 K). However, the (presumably) small size of the cluster may decrease the average strength of intermolecular interactions, thus leading to a decrease of its melting temperature. Even the formation of liquid-like outer shells with solid inner cores [16] is conceivable. Regardless of the size of the hydrogen structure in the junction, it must be noted that the enhanced imaging with its lateral resolution of $\sim$1 Å clearly shows that only one or very few hydrogen particles (molecules, atoms or protons) contribute to the imaging. A tentative schematic diagram of the STHM junction is shown in figure 3.

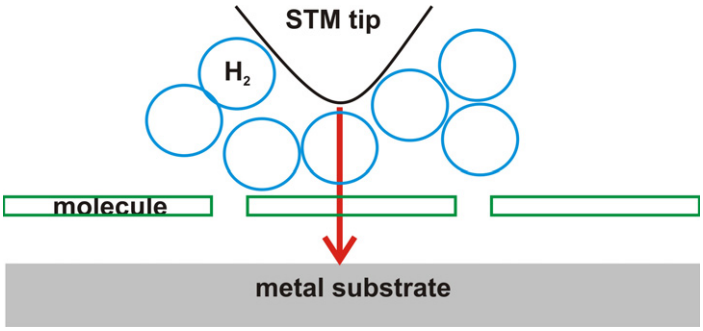

Figure 3. Tentative schematic diagram of the STHM junction.

To analyse the mechanism of the geometric image contrast in STHM further, we now turn to spectroscopic experiments with the sensitized junction. It has already been mentioned that the geometric resolution appears only at low bias voltages. This observation implies that the low bias conductance of the STM junction must change during the condensation of molecular hydrogen. As figures 4(a) and (b) demonstrate, such a change is in fact observed: a new conductance state of the junction (from now on, called conductance state 2) emerges at low bias voltages, the differential conductance of which is higher than in the original state (from now on, referred to as conductance state 1) and nonlinear. Initially, conductance state 2 appears only intermittently (cf the telegraph switching behaviour in the red and blue curves of figure 4(a)), but with increasing hydrogen condensation it turns into the stable conductance state of the junction at low bias voltages. At certain critical bias voltages (which are independent of the bias direction), a transition between the new conductance state 2 and the conventional linear conductance state 1 occurs. The transition between the two is accompanied by sharp conductance dips (i.e. negative differential resistance (NDR) features), cf figure 4(b). Comparing the tunnelling parameters that yield geometric images with those of the spectra in figure 4, it becomes clear that it is the junction operating in conductance state 2 that generates the geometric contrast, while at higher biases, the junction switches back into conductance state 1 and the conventional contrast is restored.

At this point, a note on the reproducibility of the differential conductance spectra is in order. The magenta spectrum in figure 4(b) is generic; spectra such as this are observed in the majority of cases, and they are the most stable ones. However, after some tip preparations (by which we mean the dipping of the tip into the silver surface, not covered by PTCDA or tetracene but in the presence of hydrogen), we have also observed spectra that look slightly different. For example, in rare cases the dip at zero bias was weak or missing; in other cases, a peak was even observed there. The sharp conductance features (mostly NDR dips) are always present, but both their peak energies and line shapes vary from tip preparation to tip preparation (sometimes, but less often, conductance *spikes* are observed). Tips that yield modified spectra also provide a geometric contrast, which, however, may vary from the one shown in figure 1. Similar to conventional STM, STHM may also show artefacts such as double tip effects (some of the structures in figure 1(n) may be due to this). Generally speaking, however, the variability of the images is less than that of the spectra. Overall, we can conclude that although there exists a dependence of both images and spectra on the given tip, generic features can clearly be isolated in all cases. In the following, we will restrict our discussion to the generic features of the images and spectra.

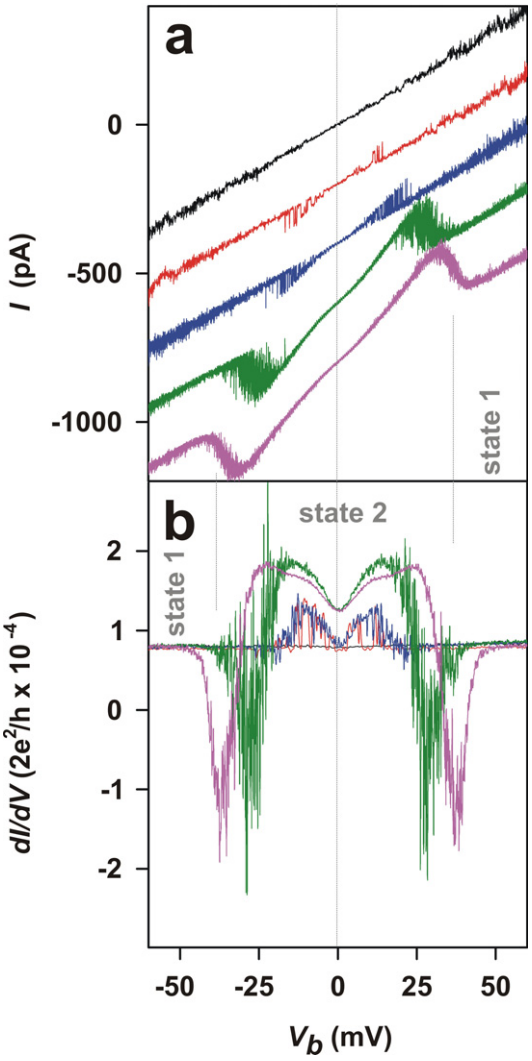

Figure 4. Spectroscopic characterization of the STM junctions. The colour sequence black–red–blue–green–magenta shows the evolution of the junction conductance during molecular hydrogen exposure. (a) Evolution of the I–V characteristics of the junction. Black: conductance spectrum in the absence of hydrogen. Red: noise in the low bias region appears as a first sign of hydrogen in the junction. After measuring the red spectrum, hydrogen exposure was stopped. Blue: the spectrum was measured 22 min after the exposure was stopped. The switching frequency has increased. Green: the spectrum was measured 80 min after the end of hydrogen exposure. Magenta: the spectrum was measured 14 h after the end of hydrogen exposure. Spectra are offset vertically (by 200 pA) for clarity. (b) $\mathrm{d}I/\mathrm{d}V$ spectra corresponding to the I–V curves shown in (a). All spectra in (a) and (b) were measured above the centre of one PTCDA molecule adsorbed on Ag(111), with the tip, which after sensitization yielded the contrast shown in figures 1(e) and (f). The stabilization point of all spectra was 0.1 nA, −0.340 V.

We note that similar sharp conductance dips (or spikes) to those observed here have been reported recently by Gupta *et al* [17] for clean metal surfaces at low temperatures in the presence of molecular hydrogen, and by Thijssen *et al* [18] for low-temperature single-molecule mechanical break junctions (Pt, Au and Ni) in the presence of molecular hydrogen or other molecules (O_2 and CO). However, neither Gupta *et al* nor Thijssen *et al* report lateral variations of the conductance and imaging applications. In accordance with our work, Gupta *et al*'s [17] spectra also depend sensitively on the tip state, the tip–surface distance and the hydrogen coverage, and after heating the STM to 25 K, hydrogen desorbs and conductance reverts to the normal behaviour. Again similar to our work, Thijssen *et al* [18] find both sharp conductance spikes and conductance dips, and a variability of the energies at which these features occur. There is a second notable feature in our spectra in figure 4, namely the dip in the conductance at zero bias which is nearly always present in our data. This zero bias anomaly (ZBA) defines a second energy scale, of the order of 5–10 meV. However, the ZBA feature is reported neither by Gupta *et al* [17] nor by Thijssen *et al* [19].

Both nonlinear features, i.e. the conductance dips/spikes (NDR) and the ZBA features, indicate that at finite bias the STHM junction shows a complex dynamical behaviour [17]–[19]. We now turn to a discussion of the nature of this dynamics. The spectra suggest that the transport electrons interact inelastically with an internal degree of freedom in the STHM junction. Since the change of conductance between the two conductance states observed in our experiments is as large as 100% and since the transition between the two conductance states is coupled to *steps in the I–V curve* (i.e. spikes or dips in $\mathrm{d}I/\mathrm{d}V$), it is unlikely that we merely observe inelastic scattering of conduction electrons as in a conventional IETS experiment (which would yield *steps in* $\mathrm{d}I/\mathrm{d}V$ at the excitation energy). Rather, the spectra point to the existence of a two-state system in which two distinct (e.g. structural) states of the junction correspond to two distinct conductance states (i.e. *state 1*/*state 2*) [17, 18]. According to this model, the inelastically scattered electrons pump energy into the junction and in this way switch the internal degree of freedom of the junction from its lower to its higher energy state. This change of the time-averaged occupation number of the two-state system may lead to abrupt steps in the *I–V* curve as a function of voltage, if it is assumed that the junction conductance in the two states of the internal degree of freedom is different. In particular, following the idea of a vibrationally induced two-level system (VITLS) [18, 20], one could imagine that tunnelling electrons excite the hydrogen in the STHM junction vibrationally. If the reaction coordinate of the vibration is collinear with the transition between the two states of the internal degree of freedom, the system can relax from the vibrationally excited state into the higher level of the two-state system, yielding a step in *I–V* (or peak in $\mathrm{d}I/\mathrm{d}V$) at the onset-energy of the relevant vibration. This mechanism would also explain the increased switching noise observed in the vicinity of the sharp conductance spikes/dips. Finally, it has been pointed out that the model of a two-state system could also exhibit a ZBA [21].

In the VITLS model, the change from the lower to the upper state of the TLS is only possible via population of a vibrational excited level the energy of which is revealed by the voltage at which the sharp conductance spikes or dips occur. Stretching vibrations of a hydrogen molecule have frequencies of the order of 400 meV [22] and thus cannot be the issue here. The lowest rotational excitation of hydrogen molecules appears around 42 meV [22], which is still larger than the typical energies of 10–30 meV observed for the NDR features in our spectra. Finally, phonon excitations of a (solid) hydrogen cluster have a typical energy of 10 meV [23]; similarly, various modes of a single hydrogen molecule embedded in a metal junction were

found to be in the range of 20–200 meV [24], the lower end of which fits our observations rather well. So it looks as if the transition between the two states of the STHM junction may be related to translational movements of hydrogen. The variability of the energies at which the transition appears is an argument in favour of the hypothesis that we may have a hydrogen cluster: a changing tip–surface distance and rising hydrogen coverage would be expected to change the shape or size of the cluster, and hence cause energy shifts of its phonon modes, too. (We note in passing, however, that for break junction experiments, a variability of the transition energies is also observed, although these junctions apparently contain only a single hydrogen molecule [18].)

As an alternative to the VITLS model, a different explanation for spectra of the type observed here has been put forward for metal nano-constrictions [25, 26]. This model is based on the two-channel Kondo (2CK) effect. However, the applicability of the 2CK model to nano-constrictions of metals is highly controversial [27]–[29]. Yet, recently it has been shown that parity-degenerate rotational states are a physical realization of 2CK physics which may well apply to nano-constrictions of metallic glasses [29], and by analogy also to the present STHM junction. The possible relationship to the geometric imaging mode of STHM will be discussed in a forthcoming publication [30]. The advantage of the 2CK scenario would be the consistent explanation of all spectral features *and* the salient features of the imaging mode itself.

Finally, we turn to a discussion of the geometric contrast mechanism itself. The first thing to note is that the *zero bias* conductance is closely linked to the geometric resolution: spectroscopic imaging of the differential conductance at various fixed bias voltages reveals that the clearest geometric resolution is obtained if the imaging is performed in the voltage range of the ZBA, in particular at zero bias, cf figure 2. For larger bias voltages approaching the conductance dips/spikes, the images acquire a very complex sub-molecular structure (not shown). Thus, we can conclude that the rapid lateral variations of the (background) conductance in the region of the ZBA (but apparently not the ZBA itself) are the key to the geometric imaging effect.

It is clear that the geometric imaging must be related to the interaction of the hydrogen in the junction with the adsorbed molecules (e.g. PTCDA or tetracene) on the surface. A key observation in this context is the fact that it is possible to image the hexagonal structure of the carbon rings, cf figure 2. This indicates that, while the hydrogen molecule or cluster in the junction follows the tip across the surface, it stays close to the local minimum of the surface corrugation potential in the middle of a C_6 ring until the tip crosses into a neighbouring ring, whence the hydrogen abruptly follows the tip, again occupying the position close to the potential minimum of the new ring. In this way, hydrogen always occupies its preferred 'adsorption' site in the middle of the ring that is closest to the tip position. The discontinuous sliding of the hydrogen-probe across the surface apparently leads to a nearly constant conductance as long as the tip apex remains within one ring, while the conductance collapses whenever the tip is located on the boundary between two rings where the probe switches between two neighbouring minima of the corrugation potential. This allows structural images of the molecules with 120° angles to be recorded. A similar behaviour has been reported for Co adatoms that are dragged across Pt(111) by a dynamic AFM tip [31]: the corresponding AFM pictures also clearly reveal the hexagonal symmetry of the Pt(111) surface.

While the above model explains the symmetry of the observed molecular images well, it does not *per se* rationalize why in some positions (e.g. inside the C_6 and, to a lesser extent, C_5O rings, and in certain positions between the molecules, which incidentally correspond to the

positions where H-bonds between the molecules form) a large zero bias conductance is found, while in other positions (e.g. between the rings and between the molecules) this conductance is much lower. This is different from the AFM experiment in [31] (including its supplement), where it is clear that the location of the Co adatom in different parts of the surface corrugation potential should lead to a contrast in the *mechanical response* of the force sensor. The question thus arises of how the lateral position of the STHM junction is related to its conductance. This issue will be addressed in a forthcoming publication [30].

The remaining theoretical uncertainties notwithstanding, we have demonstrated in this paper that in the presence of condensed hydrogen, an STM junction supports a new imaging mechanism for complex molecules. Since the ability to directly visualize the atomic structure of molecular adsorbates is extremely valuable in the research of functional interfaces, the potential of the new imaging technique is very promising. The method appears to be a true *structure* microscopy, in contrast to conventional STM, which probes electronic states. STHM achieves both a robust chemical sensitivity and a potential for molecular identification, because it relies on a molecular property that is at the same time characteristic of each molecular species *and* insensitive to the presence of the (in most cases) metallic substrate, as long as the structural integrity of the molecule is conserved on adsorption. In this sense, STHM may turn out to be superior to the other approaches suggested for chemical sensitization of the STM.

On the basis of the present data, STHM seems especially suited to carbon rings, which are so important in organic chemistry. Hence, imaging of C_{60}, carbon nanotubes (helicity!) and graphene should also work. Experiments on these systems are currently in progress. Other ring structures, even with hetero-atoms, can be visualized, too. It should be noted that according to the currently available models, the imaging method does not depend on the particular properties of hydrogen; other probe molecules, also heavier ones, may also work. It is conceivable that the conductance spectra and images contain quantitative information about the molecule which could enhance the chemical sensitivity even further. Finally, we point out that the present results once more demonstrate that STM junctions containing hydrogen reveal a complex physics [17, 19, 32] that we are only beginning to understand.

Acknowledgments

This work was financially supported by the Deutsche Forschungsgemeinschaft. It is a pleasure to thank M Sokolowski and J Kroha, both of the University of Bonn, and F B Anders, University of Bremen, for helpful discussions.

References

[1] Rosei F *et al* 2003 *Prog. Surf. Sci.* **71** 95
[2] Repp J *et al* 2005 *Phys. Rev. Lett.* **94** 026803
[3] Stipe B C, Rezaei M A and Ho W 1998 *Science* **280** 1732
[4] Neel N *et al* 2007 *Phys. Rev. Lett.* **98** 065502
[5] Temirov R *et al* 2008 *Nanotechnology* **19** 065401
[6] Kraft A *et al* 2006 *Phys. Rev.* B **74** 041402
[7] Qiu X H, Nazin G V and Ho W 2003 *Science* **299** 542
[8] Berndt R *et al* 1994 *Surf. Sci.* **309** 1033
[9] Pascual J I and Lorente N 2006 *Single-Molecule Vibrational Spectroscopy and Chemistry* ed P Grütter, W Hofer and F Rosei (Singapore: World Scientific)

[10] Pascual J I and Lorente N 2006 *Inelastic Electron Tunneling Microscopy and Spectroscopy of Single Molecules by STM* (Weinheim: Wiley-VCH)
[11] Bocquet M L, Lesnard H and Lorente N 2006 *Phys. Rev. Lett.* **96** 096101
[12] Temirov R *et al* 2006 *Nature* **444** 350
[13] Horcas I *et al* 2007 *Rev. Sci. Instrum.* **78** 013705
[14] Eremtchenko M *et al* 2005 *Phys. Rev.* B **71** 045410
[15] Ogura S *et al* 2004 *Surf. Sci.* **566–568** 755
[16] Gordillo M C and Ceperley D M 2002 *Phys. Rev.* B **65** 174527
[17] Gupta J A *et al* 2005 *Phys. Rev.* B **71** 115416
[18] Thijssen W H A *et al* 2006 *Phys. Rev. Lett.* **97** 226806
[19] Pivetta M *et al* 2007 *Phys. Rev. Lett.* **99** 126104
[20] Kozub V I and Kulik I O 1986 *Sov. Phys.—JETP* **64** 1332
[21] Kozub V I and Rudin A M 1997 *Phys. Rev.* B **55** 259
[22] Silvera I F 1980 *Rev. Mod. Phys.* **52** 393
[23] Nielsen M 1973 *Phys. Rev.* B **7** 1626
[24] Djukic D *et al* 2005 *Phys. Rev.* B **71** 161402
[25] von Delft J *et al* 1998 *Ann. Phys.* **263** 55
[26] Ralph D C and Buhrman R A 1992 *Phys. Rev. Lett.* **69** 2118
[27] Wingreen N S, Altshuler B L and Meir Y 1995 *Phys. Rev. Lett.* **75** 769
[28] Aleiner I L and Controzzi D 2002 *Phys. Rev.* B **66** 045107
[29] Arnold M, Langenbruch T and Kroha J 2007 *Phys. Rev. Lett.* **99**
[30] Temirov R *et al* 2008 *New J. Phys.* in preparation
[31] Ternes M *et al* 2008 *Science* **319** 1066
[32] Hofer W A *et al* 2008 *Phys. Rev. Lett.* **100** 026806